In Situ Transmission Electron Microscopy Probing of Native Oxide and Artificial Layers on Silicon Nanoparticles for Lithium Ion Batteries

Yang He,[‡] Daniela Molina Piper,[§] Meng Gu,[†] Jonathan J. Travis,[§] Steven M. George,[§] Se-Hee Lee,[§] Arda Genc,[∥] Lee Pullan,[∥] Jun Liu,[⊥] Scott X. Mao,[*,‡] Ji-Guang Zhang,[⊥] Chunmei Ban,[*,#] and Chongmin Wang[*,†]

[†]Environmental Molecular Sciences Laboratory, Pacific Northwest National Laboratory, 902 Battelle Boulevard, Richland, Washington 99352, United States, [‡]Department of Mechanical Engineering and Materials Science, University of Pittsburgh, 3700 O'Hara Street, Pittsburgh, Pennsylvania 15261, United States, [§]University of Colorado at Boulder, Boulder, Colorado 80309, United States, [∥]FEI Company, 5350 NE Dawson Creek Drive, Hillsboro, Oregon 97124, United States, [⊥]Energy and Environmental Directorate, Pacific Northwest National Laboratory, 902 Battelle Boulevard, Richland, Washington 99352, United States, and [#]National Renewable Energy Laboratory, 1617 Cole Boulevard, Golden, Colorado 80401, United States

ABSTRACT Surface modification of silicon nanoparticles *via* molecular layer deposition (MLD) has been recently proved to be an effective way for dramatically enhancing the cyclic performance in lithium ion batteries. However, the fundamental mechanism of how this thin layer of coating functions is not known, which is complicated by the inevitable presence of native oxide of several nanometers on the silicon nanoparticle. Using *in situ* TEM, we probed in detail the structural and chemical evolution of both uncoated and coated silicon particles upon cyclic lithiation/delithation. We discovered that upon initial lithiation, the native oxide layer converts to crystalline Li_2O islands, which essentially increases the impedance on the particle, resulting in ineffective lithiation/delithiation and therefore low Coulombic efficiency. In contrast, the alucone MLD-coated particles show extremely fast, thorough, and highly reversible lithiation behaviors, which are clarified to be associated with the mechanical flexibility and fast Li^+/e^- conductivity of the alucone coating. Surprisingly, the alucone MLD coating process chemically changes the silicon surface, essentially removing the native oxide layer, and therefore mitigates side reactions and detrimental effects of the native oxide. This study provides a vivid picture of how the MLD coating works to enhance the Coulombic efficiency, preserves capacity, and clarifies the role of the native oxide on silicon nanoparticles during cyclic lithiation and delithiation. More broadly, this work also demonstrates that the effect of the subtle chemical modification of the surface during the coating process may be of equal importance to the coating layer itself.

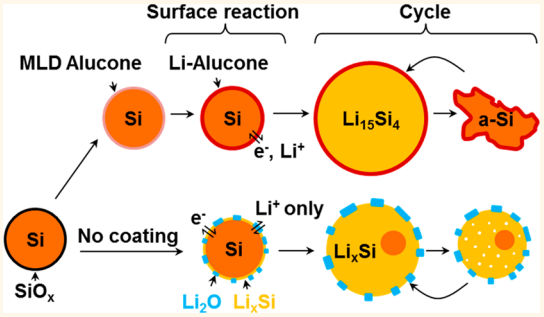

KEYWORDS: lithium ion battery · silicon nanoparticle · coating · native oxide · aluminum glycerol · *in situ* TEM

Silicon has a lithium storage capacity of 3579 mAh/g for the $Li_{15}Si_4$ final phase at room temperature. This storage capacity is almost 10 times that of commercial graphite (372 mAh/g) anodes in lithium ion batteries (LIB).[1] Extensive work has been done on exploring the possibility of using silicon as an anode for lithium ion batteries.[2] As a result of these research efforts, the intrinsic properties of silicon upon lithiation insertion and extraction have been well characterized. Among these properties is a dramatic volume change of ~300%, which gives rise to a range of electrochemimechanical effects. These effects include lithiation-induced fracture of the particle when the particle diameter is larger than a critical value of ~150 nm.[3] The drastic volume expansion and fracture result in active material disconnections from the binder and current collector, electrode film delamination, and breakup of the solid−electrolyte interface (SEI) layer.[4] These electrochemimechanical effects result in fast decaying of capacity upon cyclic reaction, which directly impedes the application of silicon as an anode for lithium ion batteries. In addition, the intrinsic existence of silicon oxide on the silicon surface induces undesirable interfacial interactions that inevitably consume lithium, leading to a chain of effects that include large first-cycle capacity

* Address correspondence to sxm2@pitt.edu; Chunmei.Ban@nrel.gov; Chongmin.Wang@pnnl.gov.

Received for review September 29, 2014 and accepted October 27, 2014.

Published online October 27, 2014
10.1021/nn505523c

loss, low specific capacity, high impedance, and incomplete lithiation.[5,6] Conversely, investigations have also shown that a relatively thick and mechanically stable oxide layer formed on the outside surface of silicon nanotubes can effectively confine the volume expansion of silicon nanotubes upon lithiation, leading to higher cycling stability.[7]

Surface modification for electrode materials has been successfully utilized to improve the cycling performance in LIB. The coating is generally perfected to function in several ways, which includes improving electric conductivity,[8] limiting or accommodating volume expansion,[8−10] preventing the particles in the electrode from isolation and agglomeration,[11,12] and modifying surface conditions for an SEI-free interface. Pioneering work in the use of aluminum oxide layers *via* atomic layer deposition (ALD) has shown the capability of Al_2O_3 ALD to stabilize highly reactive interfaces of Li-ion electrodes, effectively protecting the surface from electrolyte attack.[13−15] ALD has proven itself to be the best method to deposit continuous, conformal, and pinhole-free films at low temperatures.

Similar to the concept of ALD, most recently, molecular layer deposition (MLD) has been developed to integrate an organic backbone chain into the inorganic-based ALD films for silicon anode materials.[16] The MLD-coated silicon anodes show sustainable cycling performance with a high Coulombic efficiency above 99.9%, contrary to the fast decay observed in a bare silicon anode. Such MLD approaches enable independent manipulation of the mechanical properties of the composite electrode and the potential modification of the electronic and ionic conductivity. This manipulation allows for optimization of the mechanical integrity without sacrificing rate capability of high-energy electrodes.

The ultrathin layer of coating applied by MLD is an aluminum alkoxide hybrid organic−inorganic film fabricated using sequential, self-limited reactions between trimethylaluminum and organic alcohols, and the coating layer is termed "alucone".[17] In this case, glycerol is employed and the MLD chemistry covalently binds to the surface of the silicon particles *via* interaction with surface silanol groups. Different from physical coatings such as metals,[18,19] carbons,[20,21] and oxides,[22,23] the growth chemistry of the alucone coating can interact with the native oxide layer and builds up a 3D network of $-Al_n(-OCH_2-CHO-CH_2O-)_m$ (n:m = 1) directly on the surface of the silicon particle. The distinct electrochemical behavior of the electrode composite with MLD-coated Si anodes has been demonstrated.[16] Although the MLD coating has shown remarkable improvement in battery performance, many questions remain on how the coating (and native oxide layer) specifically works to influence the electrochemical cycling of the electrode material. Direct observation and a comparative study are needed to closely study this area.

Here, we use *in situ* transmission electron microscopy (TEM) to probe structural and chemical evolution of both the native oxide and MLD alucone-coated silicon nanoparticle upon cyclic lithiation and delithiation. We discovered that upon initial lithiation, the native oxide layer (∼2 nm in thickness) reacts with Li to form crystalline Li_2O (c-Li_2O), which partially insulates the particle during subsequent lithiation/delithiation cycles. Porous structures form upon delithiation, and a high fraction of particles investigated appear to become difficult to delithiate following the first lithiation. On the other hand, the alucone MLD coating process almost fully removed the native oxide layer. The alucone coating does not incur Li_2O formation and appears to possess great flexibility, showing compatible stretching or shrinking in accordance with the expansion or shrinkage of the silicon nanoparticles upon lithiation and delithiation. Conductivity measurements also indicate a remarkable improvement of conductivity of the lithiated alucone coating. Both reaction rate and reversible volume expansion are larger than that of native oxide-coated particles. The electrical, ionic, and mechanical characteristics of the surface-modifying alucone layers are thought to give rise to the different behaviors observed.

RESULTS AND DISCUSSION

General Structure of Pristine Si Nanoparticles with the Native Oxide Layer and MLD Alucone-Coated Si Nanoparticles. The general chemical and microstructural features of the as-received silicon nanoparticles are illustrated by the TEM images shown in Figure 1a−d. These images reveal an amorphous native oxide layer of ∼2 nm thickness overlaying the crystalline Si core. To examine the effect of the thin native oxide layer on the electron transfer properties of the particles, an $I-V$ curve was measured for a single pristine Si nanoparticle, as shown in Figure 2 (green profile). This $I-V$ curve reveals the insulating characteristics as a result of the surface native oxide layer. Similarly, an MLD alucone-coated pristine particle revealed a surface amorphous layer of ∼2 nm (Figure 1i), with the $I-V$ curve also portraying nonconductive features (Figure 2, red profile). Despite similar $I-V$ curves, the chemical composition and spatial distributions of the surface layer of the MLD-coated particle differed significantly from the uncoated pristine particles and was indeed consistent with the alucone MLD chemistry ($-Al_n(-OCH_2-CHO-CH_2O-)_m$ (n:m = 1)).

Structurally, we noticed that following the alucone coating, the thickness of the amorphous layer enclosing the silicon nanoparticle remained very similar to that of the native oxide layer on the pristine particles (Figure 1i and d, respectively). Chemically though, this amorphous alucone coating layer shows a clear dominance of Al and O, as indicated by the EDS

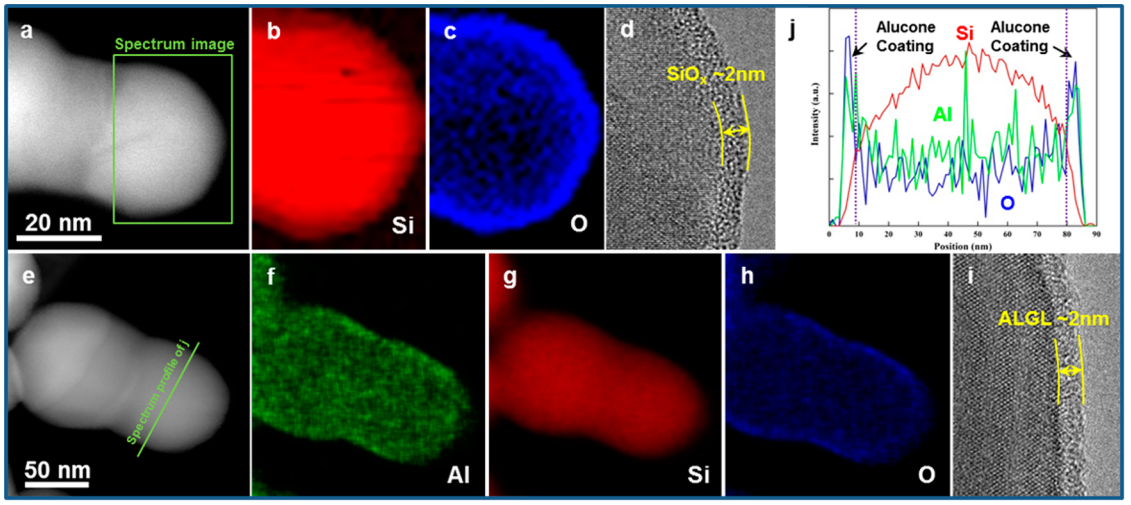

Figure 1. Morphology and element mapping of as-received (a–d) and alucone-coated Si nanoparticle (e–j), featuring a native amorphous oxide layer of ~2 nm in the as-received particle and ~2 nm alucone MLD coating in coated particle. (a) and (e) are STEM-HAADF images, (b), (c), (f), and (h) are EDS elemental maps, (d) and (i) are the HRTEM images, and (j) is a line profile across the line in (e).

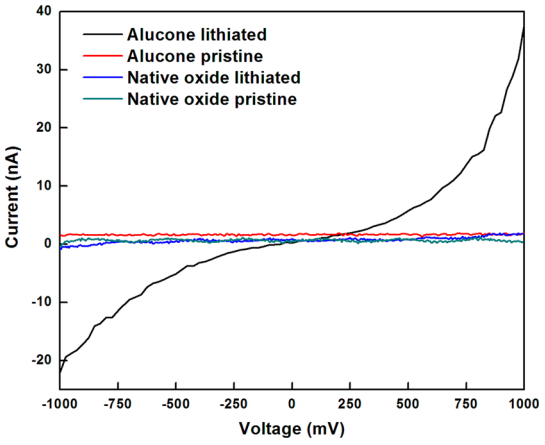

Figure 2. Conductivity of pristine and fully lithiated ($Li_{15}Si_4$ phase) native oxide-coated and alucone MLD-coated Si nanoparticles.

mapping. Note that the Al and O surface peaks are roughly of the same width (Figure 1j). These characterizations indicate that the alucone coating process removed the native oxide, in contrast to the pure physical coating model: an inner native oxide layer covered by the alucone coating layer, resulting in a thicker surface layer. Trimethylaluminum, a metal precursor used for the alucone MLD coating, is known for its ability to perform interfacial "self-cleaning" (*i.e.*, reacts with Si–O bonds) of native oxides.[24−26] The MLD precursor is also known to react with the surface silanol groups in the native SiO_x layer, as illustrated in Figure 3. Our characterization proves that these reactions greatly removed the surface native oxide layer and led to a covalently bonded and fully nucleated alucone layer on the Si particles. The fundamental details of this surface chemistry need more work and future studies.

Lithiation–Delithiation of Pristine Silicon Nanoparticles. The lithiation behavior of the pristine silicon nanoparticle is illustrated by the captured video frames shown in Figure 4 and movie S1 in the Supporting Information. The particle includes several grains separated by grain boundaries as proved by rings in the electron diffraction pattern (EDP) and HRTEM inset image (Figure 4a). Upon lithiation, grains within this particle started to swell instantaneously (arrowheads in Figure 4b). The corresponding EDP shows that crystalline silicon transforms to an amorphous lithium–silicon alloy (a-Li_xSi). The HRTEM image indicates that, upon initial lithiation, the original native oxide layer was transformed to Li_2O (Figure 3c insets).

Li_2O is intrinsically insulating[27] and conducts only Li^+ (as evidenced by the blue *I*–*V* curve of lithiated pristine particles in Figure 2). The question of how electrons go through the insulating Li_2O layer to reach the Si to allow its continuous lithiation is very intriguing. The dark-field image (Li_2O diffraction spots) indicates that the Li_2O does not form a continuous film but rather forms discrete and randomly orientated crystal islands. Between the Li_2O crystal islands, there are openings to the a-Li_xSi. These openings likely provide conductive routes for electrons.

For most of our experiments, we determined that the tested particles did not fully lithiate to the terminal $Li_{15}Si_4$ phase or fully delithiate. For example, based on the EDP in Figure 4c and volume expansion measurement (~184%), the "final" phase Li/Si ratio is ~2.3 (*i.e.*, $Li_{2.3}Si$ is far less than $Li_{3.75}Si$). In addition, the delithiated particle EDP still shows a-Li_xSi instead of a-Si features. Porous structures emerged in some particles (Figure 4d). All of these characteristics are likely associated with the impedance from the Li_2O layer, hence the slow reaction kinetics. Note that the

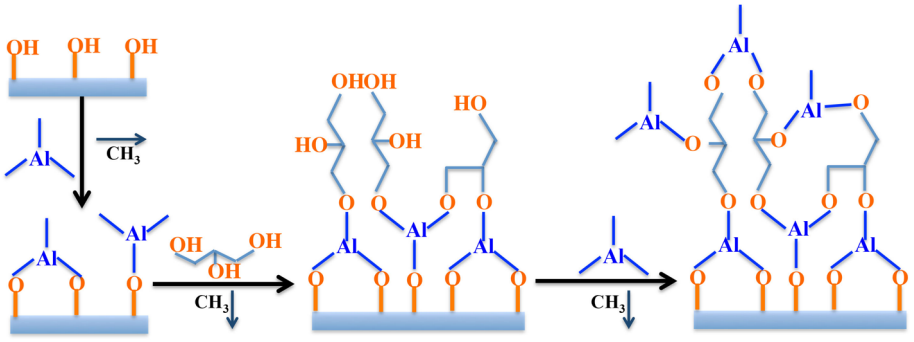

Figure 3. Schematic drawing showing the bonding of the alucone with the Si surface.

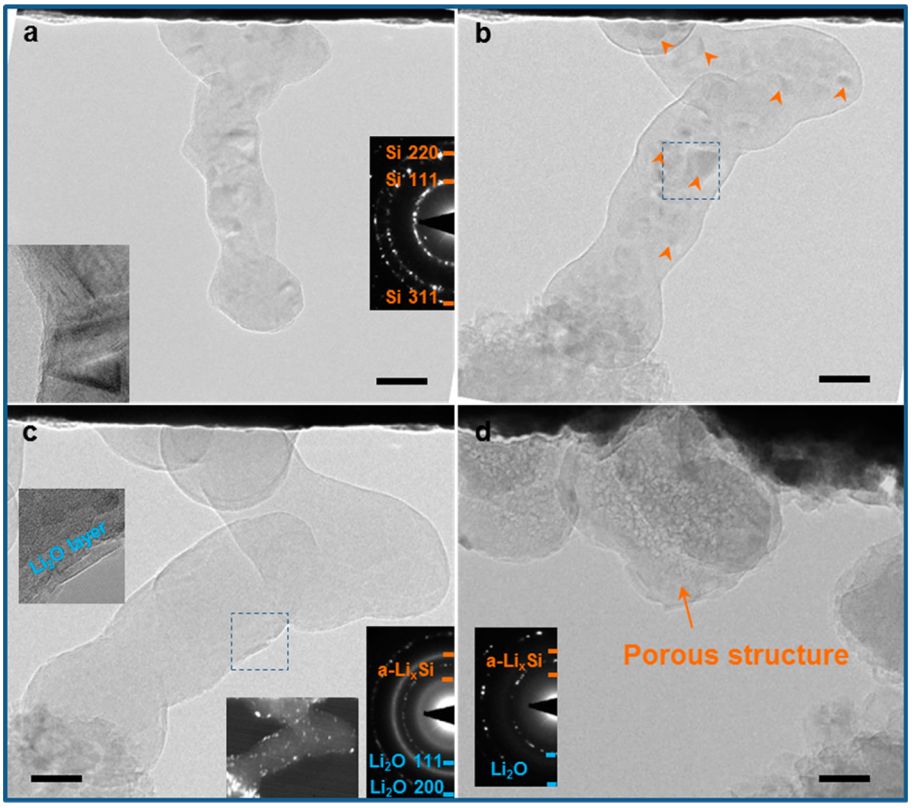

Figure 4. Captured *in situ* TEM images showing the lithiation behavior of the native oxide-coated Si nanoparticle: (a−c) pristine, mid-lithiation, and lithiated morphology. Insets are corresponding EDPs, HRTEM, and dark-field image. (d) Delithiated particles far away from the lithium source. Scale bars are 50 nm.

smaller particles lithiate faster than larger ones (Figure S3 and movie S2). This is consistent with *ex situ* electrochemical results and is associated with relatively shorter Li^+/e^- diffusion lengths in small particles.

In addition, stress has been shown to play a major role in the lithiation rate of the materials.[28,29] Li_2O is stiffer than a-Si. The rigid confinement of Li_2O islands on the surface may prevent the inward shrinkage of the particle upon delithiation, resulting in low reversible volume expansion and hence low reversible capacity.

Overall, the lithiation behavior of the bare silicon nanoparticles is characterized by the transformation of the native oxide layer SiO_x to Li_2O. The electronically insulating nature of the Li_2O layer could prevent electrons from transferring into the particle for electrochemical reactions. This could result in increased impedance and partial deactivation of active particles.

The *in situ* observations here are consistent with electrochemical tests showing detrimental effects of thermal oxide including low capacity retention, incomplete lithiation, and high impedance.[5,30] The nature of the reaction of surface oxides with Li has long been a topic of debate. Thermodynamic analysis estimates that −0.81 V *versus* Li^+/Li is needed to trigger the reaction of $SiO_2 + 4Li \rightarrow Si + 2Li_2O$.[31] Therefore, SiO_2 should remain intact in normal battery operation (0−2 V *versus* Li^+/Li). In our *in situ* TEM solid cell experiments, −2 V biasing *versus* Li^+/Li was used to drive the reaction. Thus, formation of Li_2O is reasonable.

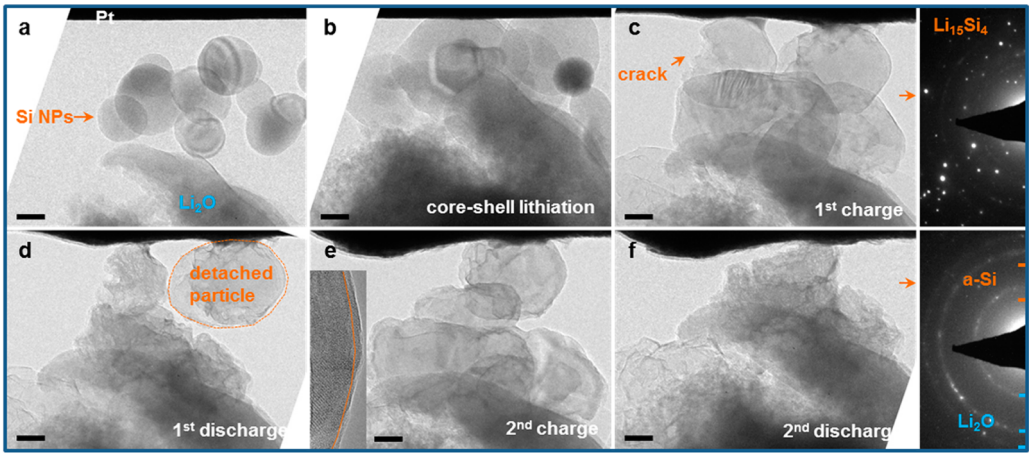

Figure 5. Captured *in situ* TEM images showing the lithiation/delithiation behavior of the alucone-coated Si nanoparticles: (a) pristine particles, (b) core−shell lithiation process, (c) after first lithiation. Arrows indicate cracks resulting from volume expansion. (d) After the first delithiation, the circled particle was detached from the congregation, indicating no agglomeration tendency. (e, f) Second lithiation and delithiation. Inset in (e) is the HRTEM of the lithiated surface showing a Li_2O-free surface. Insets on the left of (c) and (f) are corresponding EDPs showing polycrystalline $Li_{15}Si_4$ and amorphous a-Si, respectively. Scale bar is 50 nm and applies to all TEM images.

However, the nanosized native oxide layer is complicated in structure[32] and the reaction dynamics may be totally different from equilibrium thermodynamic analysis using bulk parameters of SiO_2.[33−35] *Ex situ* experiments have identified formation of Li_2O[6,34] and silicates[6,33,34] under prolonged charging at low potential (*e.g.*, 10 mV). Whether the product is intact SiO_x, lithium silicates, or Li_2O, the electrical conductivity is lower and mechanical stiffness ($E_{Li2Si2O5}$ = 135 GPa, $E_{Li4SiO4}$ = 120 GPa, E_{Li2O} = 141 GPa, E_{SiO2} = 70 GPa) is higher than that of a-Si ($E_{a\text{-}Si}$ = 80 ∓ 20 GPa), which means the electrical confinement and mechanical confinement should work in the same manner. Although the voltage used is below the voltage window in a real battery, it is reasonable that native oxide will impose the same effect as observed here.

Lithiation−Delithiation of Alucone MLD-Coated Silicon Nanoparticles. The lithiation and delithiation characteristics of the alucone-coated silicon particles are revealed by sequential TEM images in Figure 5 and movie S3 in the Supporting Information. The particles started lithiation from the surface, forming a core−shell structure. Within 18 s, the particles reached a full lithiation state of the $Li_{15}Si_4$ phase, as verified by the corresponding EDP. Unlike the pristine particles, there is no Li_2O formed on the surface of alucone-coated particles due to the removal of the SiO_x during the MLD-coating process (Figure 3). The HRTEM image reveals the Li_2O-free surface of the MLD-coated particles (Figure 5e inset).

Upon delithiation (movie S3), together with the surface MLD coating, the particles remarkably shrank with no pore formation or coating delamination. In 50 s, the particles delithiated to the final state of a-Si, as verified by the corresponding EDP. The same "balloon-like" behaviors were repeated in the subsequent lithiation and delithiation cycles (Figure 5e,f, movie S3) and repeated experiments. These observations dramatically diverge from the case of the pristine silicon nanoparticle in two major ways. First, the reversible volume change (or reversible capacity) of the MLD-coated particle was much larger, which happened between a-Si and $Li_{15}Si_4$. Compared to the high Young's modulus of SiO_2 and Li_2O, the low Young's modulus of the alucone MLD coating ($E_{alucone} \approx 32$ GPa) ensures the concordant deformation of the surface coating and Si particle. Second, the reaction kinetics was much faster for the coated particles than the pristine ones (compare movies S1/2 and S3), which implies that the MLD coating conducts Li^+ ions. Meanwhile, *in situ* measurement shows that electric conductivity of an alucone MLD-coated particle remarkably improved after the first lithiation (Figure 2, black profile). It should be pointed out that both electric and ionic conductivity are required for sustainable electrochemical performance. Among electric conductive coatings, the carbon coating has been widely used to improve the cycling stability for both anodes and cathodes. The result of this work indicates that the alucone coating leads to both electrical and ionic conductivity, which is of a key reason why the alucone-modified silicon particles show greater cyclability than uncoated particles.

Above all, the mechanical flexibility and good Li^+/e^- conductivity eliminate mechanical and electrical confinement of the native oxide, enabling fast and thorough electrochemical reactions of the Si particles. Figure 6 and movie S4 show high-resolution TEM images of the lithiation process of alucone-coat Si. Lithiation starts from the alucone layer and gradually proceeds inward, leading to the formation of a multicore−shell configuration, as illustrated in Figure 6d. Upon lithiation, the thickness of the alucone MLD coating changes from ~1.7 nm to ~3 nm. Consistent with all other observations of

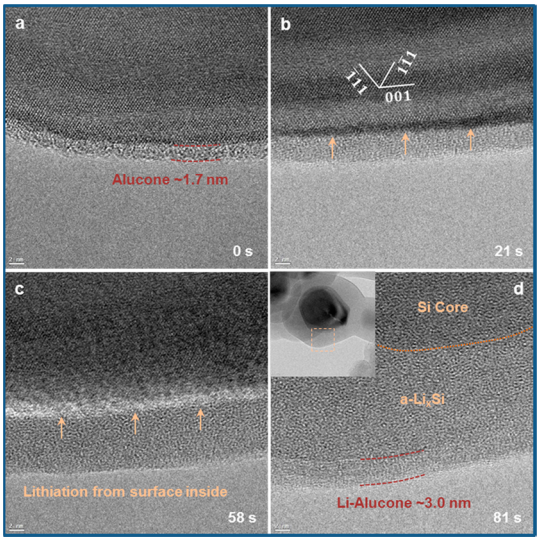

Figure 6. Captured *in situ* HRTEM image revealing details of the alucone-coated Si nanoparticle lithiation process. Arrows indicate the reaction front.

alucone-coated particles, no crystalline Li_2O is detected. The phase of the amorphous lithiated alucone is difficult to determine.

Although it is difficult to quantify, we noticed that lithiation of native oxide-coated Si particles shows a tendency toward interparticle welding when two particles are impinged spatially (Figure S3 and movie S2), as similarly observed in previous studies.[11,36] However, following the alucone coating, such impingement-induced welding is mitigated, as illustrated in Figure 5d by the circled particle. Particle augmentation requires interparticle atomic transport. For the case of the native oxide-covered particle, the lithiation-induced transformation of SiO_x to Li_2O is a process that can be affiliated with Si atomic transport. A lack of interparticle welding indicates that Si atoms are hard to diffuse or transport through the alucone layer. The mitigation of the particle welding (or agglomeration) also contributes to the enhanced cycling performance observed with the alucone-coated Si particles.

General Discussions. Native oxide layers of several nanometers thick inevitably exist on metal and semiconductor nanoparticles. The role of such a thin native oxide layer is very well perceived and beneficially utilized, such as on stainless steel.[37] Although massive amounts of work have been done with respect to the electrochemical characteristics of Si nanoparticles as an anode for lithium ion batteries, the role of the thin native oxide layer on the Si nanoparticle surface has previously never been clarified. This work presents a comparative study, on a single-particle scale, of the electrochemical behavior of the native oxide layer and artificial alucone MLD coating (without native oxide) on Si nanoparticles and emphasizes the significance of surface engineering strategy in improving electrochemical performances.

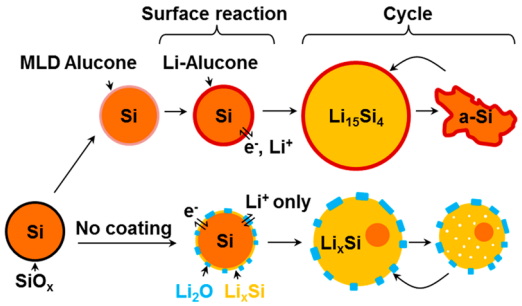

Figure 7. Schematics of surface reactions and cycle behaviors of silicon nanoparticles with different coating conditions.

The observed effects of the native oxide layer and the alucone coating on the behavior of particles are schematically summarized in Figure 7. The native oxide on Si transforms to a Li_2O layer upon lithiation at low potentials (*e.g.*, −2 V *vs* Li^+/Li). This Li_2O layer poses electrical and mechanical confinement to the particle, retarding desirable electrochemical reactions and insulating active particles. As discussed in the above sections, these effects exist for all possible reaction products of the surface native oxide. A conventional physical coating preserving the native oxide layer cannot circumvent these effects. Conversely, the alucone MLD coating cleans the surface native oxide layer, thus eliminating the effects of native oxide, and possesses great mechanical flexibility and Li^+/e^- conductivity upon initial lithiation. The good conductivity enables faster, complete electrochemical reactions and high rate performance. The remarkable mechanical flexibility of the alucone layer enabled a concordant response to the volume change of silicon during the lithiation and delithiation. The alucone layer maintained the integrity of the contacted particle, as similarly demonstrated for stretchable polymers.[9] Due to the setup of the *in situ* experiment, a Li_2O solid electrolyte was used and an overpotential is normally applied. Therefore, the correlation of the voltage and reaction cannot be directly related to battery operation. However, the above discussion on possible surface reaction products proves that the structural evolution of the uncoated and coated particle captured by the *in situ* TEM should essentially be the same as what happens in the lithium ion battery.

In this study, the coating layer effect has been mostly evaluated from the point of the view of the coating layer itself. The present observation of the removal of the native oxide layer during the alucone coating likely implies that the application of the coating layer may also modify the surface structure and chemistry of the nanoparticles. This oxide removal passivates unwanted and irreversible charge losses resulting from native oxide. The positive effects observed from the surface modification of the alucone coating on Si nanoparticles on the electrochemical

properties suggest a possible major technological advancement for lithium ion batteries.

CONCLUSIONS

The native oxide layer on Si anodes will create Li_2O upon lithiation. The role of the Li_2O layer on charge−discharge cycles can be evaluated from both electrical and mechanical effect. The electrical effect originates from its insulating nature of native oxide and Li_2O, which may induce the deactivation of particles. The mechanical confinement of Li_2O originates from its higher stiffness than silicon and contributes to incomplete delithiation. On the other hand, alucone MLD-coating process consumes SiO_x, avoids formation of Li_2O, and is mechanically flexible and electron/Li^+ conductive after lithiation. These features of alucone MLD coating effectively facilitate fast and thorough reversible electrochemical reactions. For the Si particle with a size above a critical dimension, the drastic volume change may induce stresses that can still crack the SEI layer, contributing to capacity losses in the first few cycles. Above all, our findings demonstrated the effect of alucone MLD coating and the native oxide layer on the lithiation−delithiation process of silicon nanoparticles, providing critical guidance to coating designs for improved cycling performance.

METHODS

The silicon nanoparticle used in this work and the fabrication process of the alucone coating layer on the silicon nanoparticle were described in detail in a prior paper.[16] In brief, alucone coatings were grown directly on the nano-Si material using the sequential reactions of trimethylaluminum and glycerol. The typical growth rate for the alucone chemistry is 2.5 Å per cycle, and all of the coating reactions were conducted at 140 °C.

The coating layer structure and chemcial composition were examined by high-resoution transmission electron microscopy (HRTEM) imaging and energy dispersive X-ray spectroscopy anlysis (EDS). The EDS was carried out on a scanning TEM (S/TEM) with 200 kV acceleration voltage and fitted with four silicon drifted detectors. Due to increased EDS collection efficiency, a large-size EDS map can be obtained faster, therefore reducing the artifact associated with the sample drift during the analysis. HRTEM images were acquired using Titan80-300 fitted with an imaging-lens corrector and operated at 300 kV.

The *in situ* TEM observations of the lithiation and delithiation of the particles were carried out using an open cell configuration as schematically illustrated in Figure S1. The silicon particles were loaded on a Pt rod, which is fixed on one side of the TEM holder (Nanofactory STM). Lithium metal is loaded on a W rod, which is navigated by a piezoelectric system on the other side of the holder. Lithium metal is driven to contact the silicon particles. The lithium oxide layer on the lithium metal surface serves as an electrolyte. In order to drive Li^+ diffusion in Li_2O, an overpotential of −2 V is applied on Si against the Li metal to lithiate the Si. The microstructure changes were recorded using a charge-couple device (CCD) attached to the TEM. For the *in situ* conductivity measurement (Figure S2), a single particle was loaded on the W probe opposing the double-tip-Pt rod with Li metal (for lithiation) and fresh Pt surface (for the *in situ* conductivity measurement). This setup gurantees good contact and avoids air-exposure. The Pt surface was driven to contact the particle after the first lithiation for conductivity measurement.

Conflict of Interest: The authors declare no competing financial interest.

Acknowledgment. This work at PNNL and NREL is supported by the Assistant Secretary for Energy Efficiency and Renewable Energy, Office of Vehicle Technologies of the U.S. Department of Energy under Contract No. DE-AC02-05CH11231, Subcontract No. 18769 and DE-AC-36-08GO28308 under the Batteries for Advanced Transportation Technologies program. The *in situ* microscopic study described in this paper is supported by the Laboratory Directed Research and Development Program as part of the Chemical Imaging Initiative at Pacific Northwest National Laboratory (PNNL). The work was conducted in the William R. Wiley Environmental Molecular Sciences Laboratory (EMSL), a national scientific user facility sponsored by DOE's Office of Biological and Environmental Research and located at PNNL. PNNL is operated by Battelle for the DOE under Contract DE-AC05-76RLO1830.

Supporting Information Available: The Supporting Information includes schematics of the solid cell setup, demonstration of *in situ* conductivity measurements, and extra experimental data on native oxide-coated Si nanoparticles. Movies on cyclic behavior of native oxide-coated nanoparticles (movies S1 and S2) and alucone MLD-coated nanoparticles (movies S3 and S4) are also included. This material is available free of charge *via* the Internet at http://pubs.acs.org.

REFERENCES AND NOTES

1. Liu, X. H.; Huang, J. Y. *In Situ* TEM Electrochemistry of Anode Materials Iin Lithium Ion Batteries. *Energy Environ. Sci.* **2011**, *4*, 3844–3860.
2. Chan, C. K.; Peng, H.; Liu, G.; Mcllwrath, K.; Zhang, X. F.; Huggins, R. A.; Cui, Y. High-Performance Lithium Battery Anodes Using Silicon Nanowires. *Nat. Nanotechnol.* **2008**, *3*, 31–35.
3. Liu, X. H.; Zhong, L.; Huang, S.; Mao, S. X.; Zhu, T.; Huang, J. Y. Size-Dependent Fracture of Silicon Nanoparticles during Lithiation. *ACS Nano* **2012**, *6*, 1522–1531.
4. Wu, J. J.; Bennett, W. R. In *Fundamental Investigation of Si Anode in Li-Ion Cells*; Energytech, 2012 IEEE, May 29−31, 2012; **2012**; pp 1−5.
5. Xun, S.; Song, X.; Wang, L.; Grass, M. E.; Liu, Z.; Battaglia, V. S.; Liu, G. The Effects of Native Oxide Surface Layer on the Electrochemical Performance of Si Nanoparticle-Based Electrodes. *J. Electrochem. Soc.* **2011**, *158*, A1260–A1266.
6. Nagao, Y.; Sakaguchi, H.; Honda, H.; Fukunaga, T.; Esaka, T. Structural Analysis of Pure and Electrochemically Lithiated SiO Using Neutron Elastic Scattering. *J. Electrochem. Soc.* **2004**, *151*, A1572–A1575.
7. Wu, H.; Chan, G.; Choi, J. W.; Ryu, I.; Yao, Y.; McDowell, M. T.; Lee, S. W.; Jackson, A.; Yang, Y.; Hu, L.; *et al.* Stable Cycling of Double-Walled Silicon Nanotube Battery Anodes through Solid-Electrolyte Interphase Control. *Nat. Nanotechnol* **2012**, *7*, 310–315.
8. Zhang, L. Q.; Liu, X. H.; Liu, Y.; Huang, S.; Zhu, T.; Gui, L. J.; Mao, S. X.; Ye, Z. Z.; Wang, C. M.; Sullivan, J. P.; *et al.* Controlling the Lithiation-Induced Strain and Charging Rate in Nanowire Electrodes by Coating. *ACS Nano* **2011**, *5*, 4800–4809.
9. Wang, C.; Wu, H.; Chen, Z.; McDowell, M. T.; Cui, Y.; Bao, Z. N. Self-Healing Chemistry Enables the Stable Operation of Silicon Microparticle Anodes for High-Energy Lithium-ion Batteries. *Nat. Chem.* **2013**, *5*, 1042–1048.
10. Liu, Y.; Hudak, N. S.; Huber, D. L.; Limmer, S. J.; Sullivan, J. P.; Huang, J. Y. *In Situ* Transmission Electron Microscopy Observation of Pulverization of Aluminum Nanowires and Evolution of the Thin Surface Al_2O_3 Layers during Lithiation-Delithiation Cycles. *Nano Lett.* **2011**, *11*, 4188–4194.

11. Karki, K.; Epstein, E.; Cho, J. H.; Jia, Z.; Li, T.; Picraux, S. T.; Wang, C.; Cumings, J. Lithium-Assisted Electrochemical Welding in Silicon Nanowire Battery Electrodes. *Nano Lett.* **2012**, *12*, 1392–1397.
12. Liu, N.; Wu, H.; McDowell, M. T.; Yao, Y.; Wang, C.; Cui, Y. A Yolk-Shell Design for Stabilized and Scalable Li-ion Battery Alloy Anodes. *Nano Lett.* **2012**, *12*, 3315–3321.
13. Leung, K.; Qi, Y.; Zavadil, K. R.; Jung, Y. S.; Dillon, A. C.; Cavanagh, A. S.; Lee, S. H.; George, S. M. Using Atomic Layer Deposition to Hinder Solvent Decomposition In Lithium Ion Batteries: First-Principles Modeling And Experimental Studies. *J. Am. Chem. Soc.* **2011**, *133*, 14741–14754.
14. Jung, Y. S.; Cavanagh, A. S.; Dillon, A. C.; Groner, M. D.; George, S. M.; Lee, S.-H. Enhanced Stability of $LiCoO_2$ Cathodes in Lithium-Ion Batteries Using Surface Modification by Atomic Layer Deposition. *J. Electrochem. Soc.* **2010**, *157*, A75–A81.
15. Jung, Y. S.; Lu, P.; Cavanagh, A. S.; Ban, C.; Kim, G.-H.; Lee, S.-H.; George, S. M.; Harris, S. J.; Dillon, A. C. Unexpected Improved Performance of ALD Coated LiCoO2/Graphite Li-Ion Batteries. *Adv. Energy Mater.* **2013**, *3*, 213–219.
16. Piper, D. M.; Travis, J. J.; Young, M.; Son, S. B.; Kim, S. C.; Oh, K. H.; George, S. M.; Ban, C. M.; Lee, S. H. Reversible High-Capacity Si Nanocomposite Anodes for Lithium-ion Batteries Enabled by Molecular Layer Deposition. *Adv. Mater.* **2013**, *26*, 1596–1601.
17. Dameron, A. A.; Seghete, D.; Burton, B. B.; Davidson, S. D.; Cavanagh, A. S.; Bertrand, J. A.; George, S. M. Molecular Layer Deposition of Alucone Polymer Films Using Trimethylaluminum and Ethylene Glycol. *Chem. Mater.* **2008**, *20*, 3315–3326.
18. Sethuraman, V. A.; Kowolik, K.; Srinivasan, V. Increased Cycling Efficiency and Rate Capability of Copper-Coated Silicon Anodes in Lithium-Ion Batteries. *J. Power Sources* **2011**, *196*, 393–398.
19. Yu, Y.; Gu, L.; Zhu, C.; Tsukimoto, S.; van Aken, P. A.; Maier, J. Reversible Storage of Lithium in Silver-Coated Three-Dimensional Macroporous Silicon. *Adv. Mater.* **2010**, *22*, 2247–2250.
20. Luo, J.; Zhao, X.; Wu, J.; Jang, H. D.; Kung, H. H.; Huang, J. Crumpled Graphene-Encapsulated Si Nanoparticles for Lithium Ion Battery Anodes. *J. Phys. Chem. Lett.* **2012**, *3*, 1824–1829.
21. Ng, S. H.; Wang, J.; Wexler, D.; Konstantinov, K.; Guo, Z. P.; Liu, H. K. Highly Reversible Lithium Storage In Spheroidal Carbon-Coated Silicon Nanocomposites as Anodes for Lithium-Ion Batteries. *Angew. Chem., Int. Ed.* **2006**, *45*, 6896–4899.
22. Jung, S. C.; Han, Y.-K. How Do Li Atoms Pass through the Al_2O_3 Coating Layer during Lithiation in Li-ion Batteries? *J. Phys. Chem. Lett.* **2013**, *4*, 2681–2685.
23. He, Y.; Yu, X.; Wang, Y.; Li, H.; Huang, X. Alumina-Coated Patterned Amorphous Silicon as the Anode for a Lithium-Ion Battery with High Coulombic Efficiency. *Adv. Mater.* **2011**, *23*, 4938–4941.
24. Hinkle, C. L.; Sonnet, A. M.; Vogel, E. M.; McDonnell, S.; Hughes, G. J.; Milojevic, M.; Lee, B.; Aguirre-Tostado, F. S.; Choi, K. J.; Kim, H. C.; *et al*. GaAs Interfacial Self-Cleaning by Atomic Layer Deposition. *Appl. Phys. Lett.* **2008**, *92*, 071901.
25. Hou, C. H.; Chen, M. C.; Chang, C. H.; Wu, T. B.; Chiang, C. D.; Luo, J. J. Effects of Surface Treatments on Interfacial Self-Cleaning in Atomic Layer Deposition of Al_2O_3 on InSb. *J. Electrochem. Soc.* **2008**, *155*, G180–G183.
26. Puurunen, R. L. Surface Chemistry of Atomic Layer Deposition: A Case Study for the Trimethylaluminum/Water Process. *J. Appl. Phys.* **2005**, *97*, 121301.
27. Radin, M. D.; Rodriguez, J. F.; Tian, F.; Siegel, D. J. Lithium Peroxide Surfaces Are Metallic, while Lithium Oxide Surfaces Are Not. *J. Am. Chem. Soc.* **2012**, *134*, 1093–103.
28. Zhao, K.; Pharr, M.; Wan, Q.; Wang, W. L.; Kaxiras, E.; Vlassak, J. J.; Suo, Z. Concurrent Reaction and Plasticity during Initial Lithiation of Crystalline Silicon in Lithium-Ion Batteries. *J. Electrochem. Soc.* **2012**, *159*, A238–A243.
29. Gu, M.; Yang, H.; Perea, D. E.; Zhang, J. G.; Zhang, S.; Wang, C. M. Bending-Induced Symmetry Breaking of Lithiation in Germanium Nanowires. *Nano Lett.* **2014**, *14*, 4622–4627.
30. Yang, J.; Takeda, Y.; Imanishi, N.; Capiglia, C.; Xie, J. Y.; Yamamoto, O. SiOx-Based Anodes for Secondary Lithium Batteries. *Solid State Ionics* **2002**, *152*, 125–129.
31. Saint, J.; Morcrette, M.; Larcher, D.; Laffont, L.; Beattie, S.; Pérès, J. P.; Talaga, D.; Couzi, M.; Tarascon, J. M. Towards a Fundamental Understanding of the Improved Electrochemical Performance of Silicon–Carbon Composites. *Adv. Funct. Mater.* **2007**, *17*, 1765–1774.
32. Choi, N.-S.; Yew, K. H.; Lee, K. Y.; Sung, M.; Kim, H.; Kim, S.-S. Effect of Fluoroethylene Carbonate Additive on Interfacial Properties of Silicon Thin-Film Electrode. *J. Power Sources* **2006**, *161*, 1254–1259.
33. Sun, Q.; Zhang, B.; Fu, Z.-W. Lithium Electrochemistry of SiO_2 Thin Film Electrode for Lithium-Ion Batteries. *Appl. Surf. Sci.* **2008**, *254*, 3774–3779.
34. Miyachi, M.; Yamamoto, H.; Kawai, H.; Ohta, T.; Shirakata, M. Analysis of SiO Anodes for Lithium-Ion Batteries. *J. Electrochem. Soc.* **2005**, *152*, A2089–A2091.
35. Ban, C.; Kappes, B. B.; Xu, Q.; Engtrakul, C.; Ciobanu, C. V.; Dillon, A. C.; Zhao, Y. Lithiation of Silica through Partial Reduction. *Appl. Phys. Lett.* **2012**, *100*, 243905.
36. Gu, M.; Li, Y.; Li, X. L.; Hu, S. Y.; Zhang, X. W.; Xu, W.; Thevuthasan, S.; Baer, D. R.; Zhang, J. G.; Liu, J.; *et al*. *In Situ* TEM Study of Lithiation Behavior of Silicon Nanoparticles Attached to and Embeded in a Carbon Matrix. *ACS Nano* **2012**, *6*, 8439–8447.
37. Atkinson, A. Transport Processes during the Growth of Oxide Films at Elevated Temperature. *Rev. Mod. Phys.* **1985**, *57*, 437–470.